

Moire Physics in Semiconductors

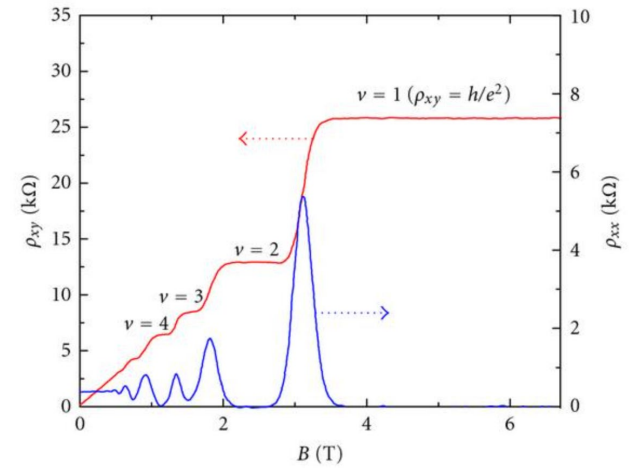
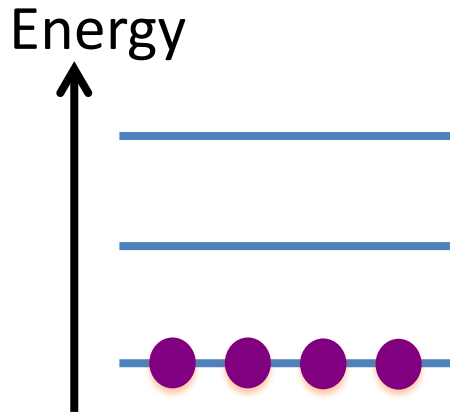
Topology with and without Flat Bands

Liang Fu

2023 Theory Winter School at MagLab

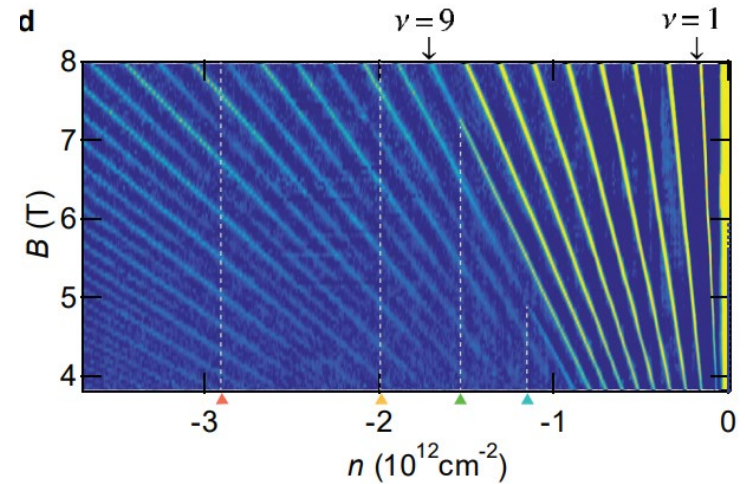


Landau Levels



$$\sigma_{xy} = N \frac{e^2}{h}$$

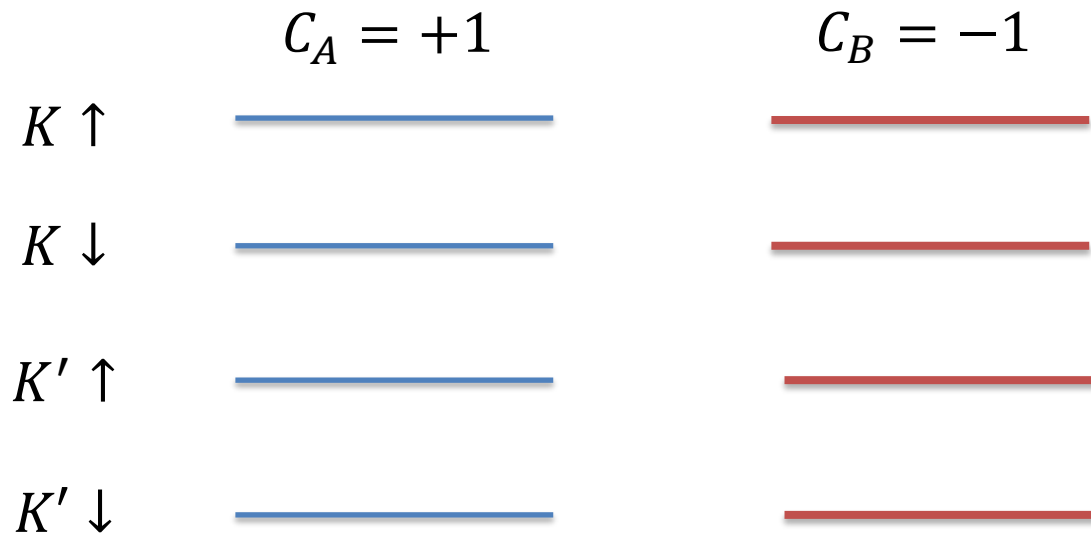
$$\frac{dn}{dB} = N \frac{e}{h}$$



Magic-Angle Twisted Bilayer Graphene

flat band from Dirac fermion with spatially varying interlayer tunneling (AA, BB, AB, BA)

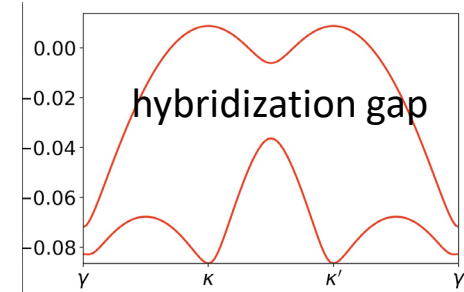
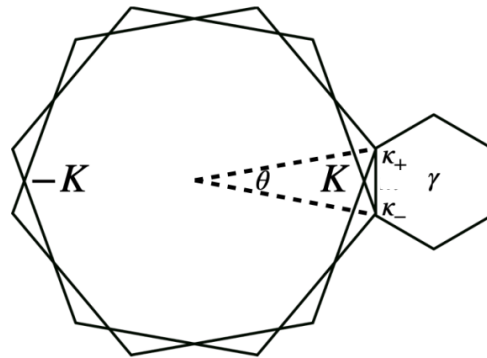
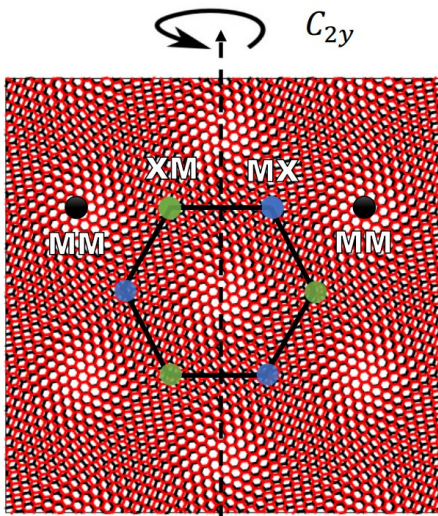
chiral limit: 8 flat Chern bands at $E = 0$



Topological Insulators in Twisted Transition Metal Dichalcogenide Homobilayers

Fengcheng Wu,^{1,2} Timothy Lovorn,³ Emanuel Tutuc,⁴ Ivar Martin,¹ and A. H. MacDonald³

$\theta \sim 0$ (AA stacking)



$$\mathcal{H}_{\uparrow} = \begin{pmatrix} -\frac{\hbar^2(\mathbf{k}-\boldsymbol{\kappa}_+)^2}{2m^*} + \Delta_b(\mathbf{r}) & \Delta_T(\mathbf{r}) \\ \Delta_T^\dagger(\mathbf{r}) & -\frac{\hbar^2(\mathbf{k}-\boldsymbol{\kappa}_-)^2}{2m^*} + \Delta_t(\mathbf{r}) \end{pmatrix}$$

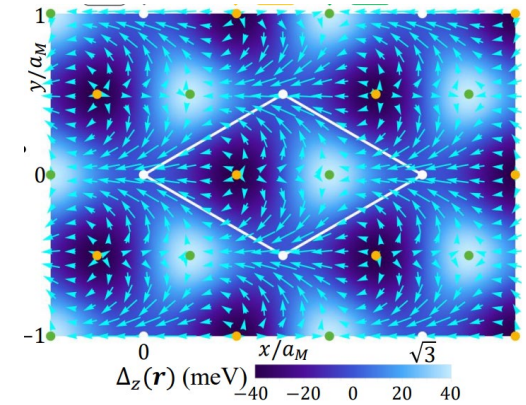
$$\Delta(\mathbf{r}) = (\Delta_x, \Delta_y, \Delta_z) \equiv (\text{Re}\Delta_T^\dagger, \text{Im}\Delta_T^\dagger, \frac{\Delta_b - \Delta_t}{2})$$

- moire potential $V(\mathbf{r})$ and complex-valued interlayer tunneling $w(\mathbf{r})$
- $w(\mathbf{r})$ vanishes at XM & MX due to atomic-scale interference of K-point w.f.

Band Topology from Skrymion Lattice

$$\mathcal{H}_\uparrow = \begin{pmatrix} -\frac{\hbar^2(\mathbf{k}-\boldsymbol{\kappa}_+)^2}{2m^*} + \Delta_b(\mathbf{r}) & \Delta_T(\mathbf{r}) \\ \Delta_T^\dagger(\mathbf{r}) & -\frac{\hbar^2(\mathbf{k}-\boldsymbol{\kappa}_-)^2}{2m^*} + \Delta_t(\mathbf{r}) \end{pmatrix}$$

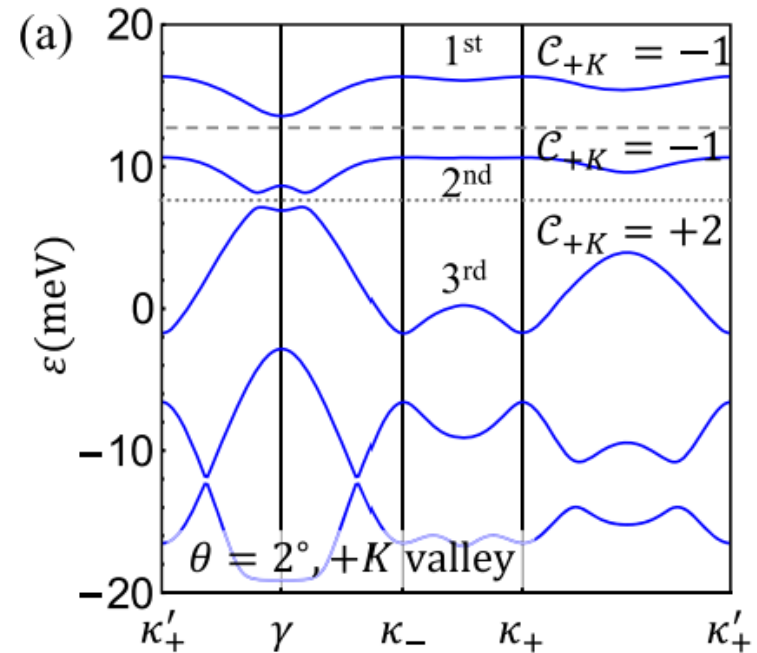
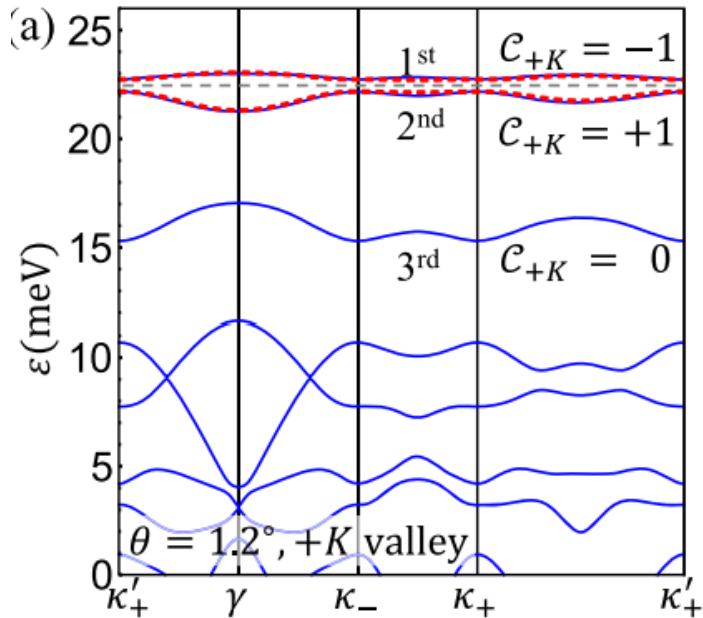
$$\boldsymbol{\Delta}(\mathbf{r}) = (\Delta_x, \Delta_y, \Delta_z) \equiv (\text{Re}\Delta_T^\dagger, \text{Im}\Delta_T^\dagger, \frac{\Delta_b - \Delta_t}{2})$$



Layer-pseudospin Zeeman field forms skrymion lattice!

Wu, Lovorn, Tutuc, Martin and MacDonald, PRL (2019)

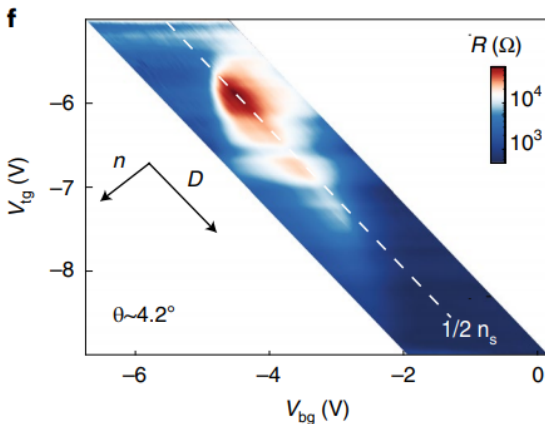
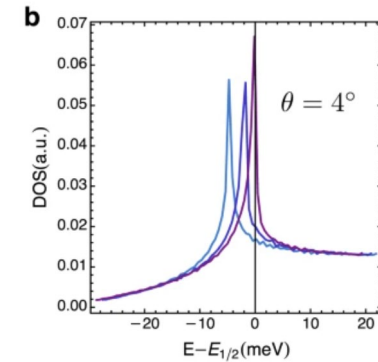
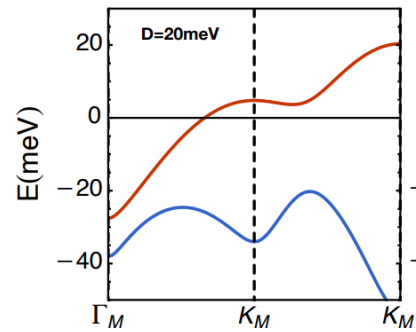
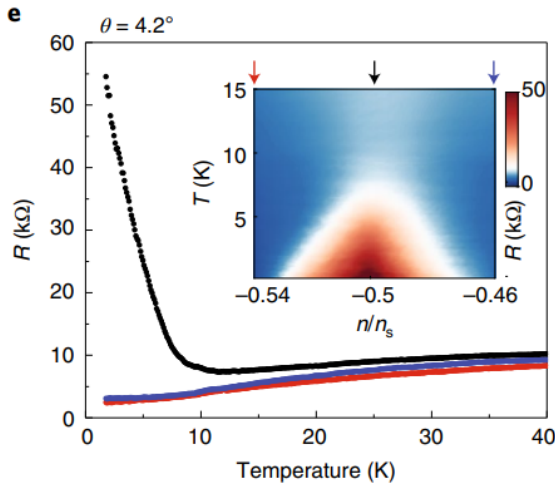
Band Topology from Skrymion Lattice



Wu, Lovorn, Tutuc, Martin and MacDonald, PRL (2019)

Twisted WSe_2 at $\theta \sim 4^\circ$

Metal-insulator transition tuned by E field

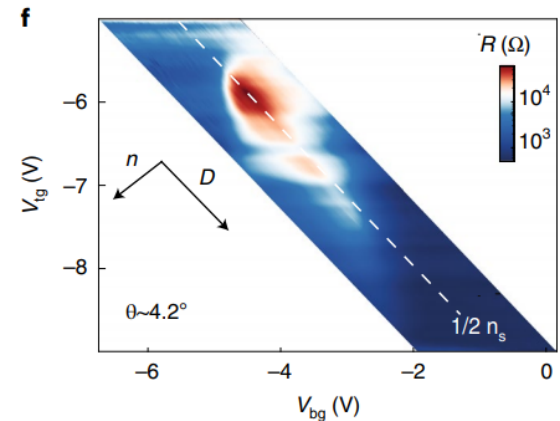
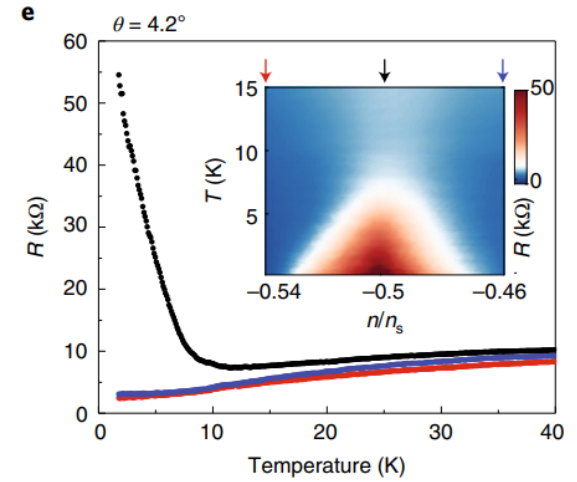
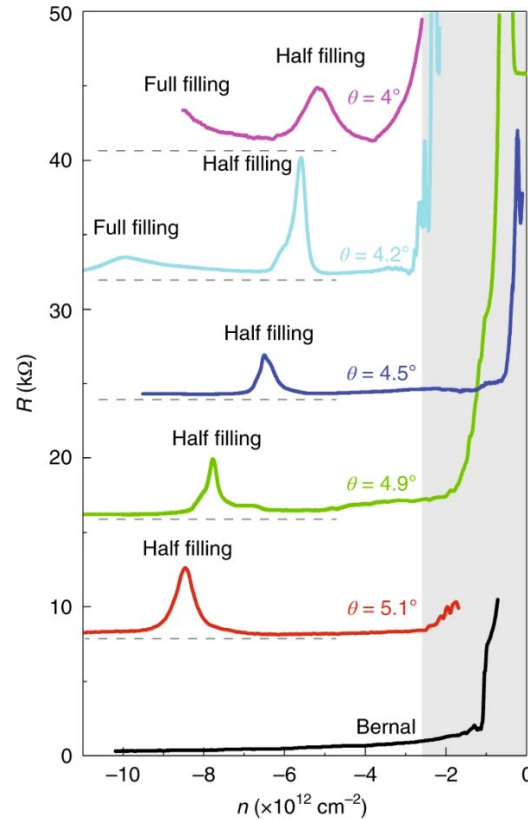
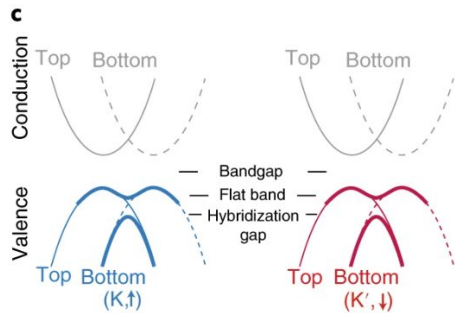
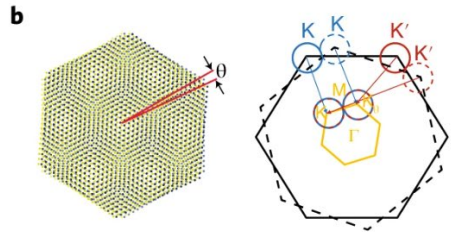
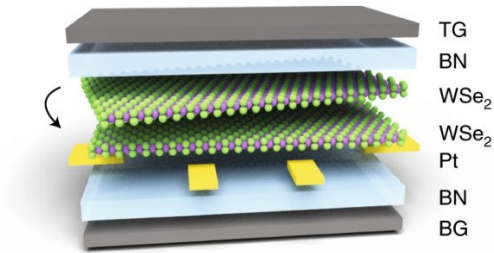


Correlated insulator at $n=1$:

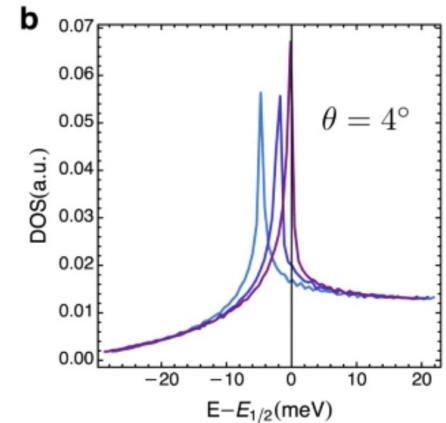
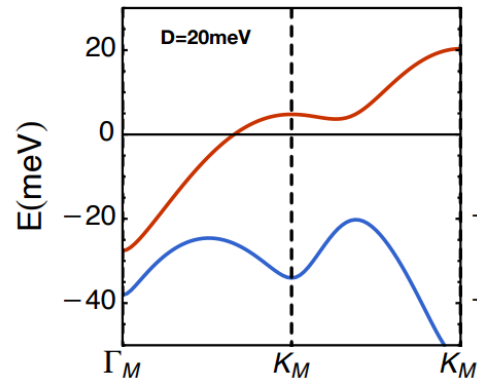
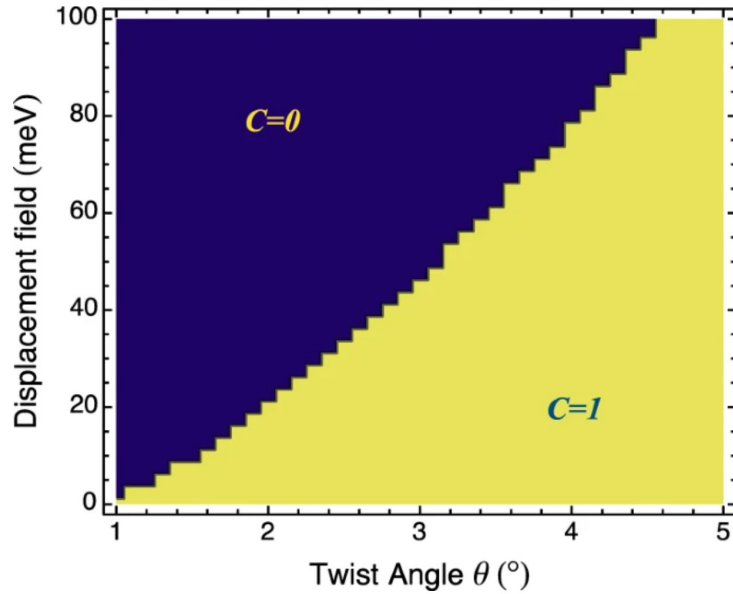
- valley-polarized (Ising) ferromagnet
- intervalley coherent (xy) antiferromagnet

Twisted WSe₂ at $\theta \sim 4^\circ$

Metal-insulator transition tuned by E field



Twisted WSe₂

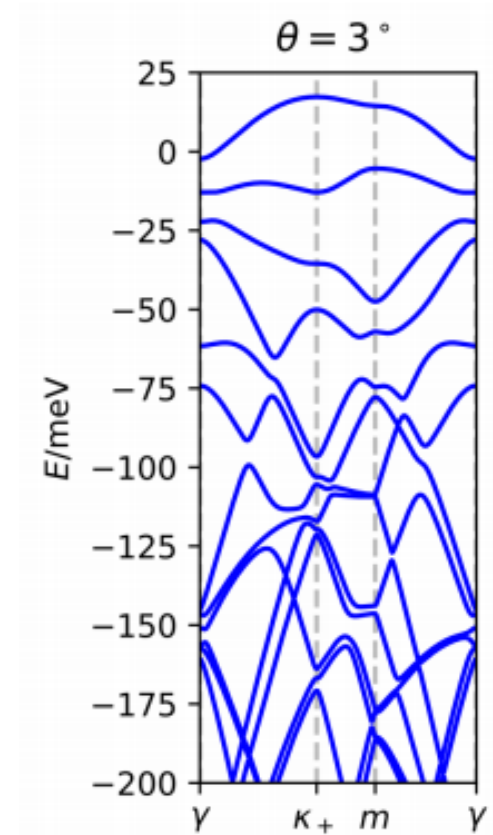
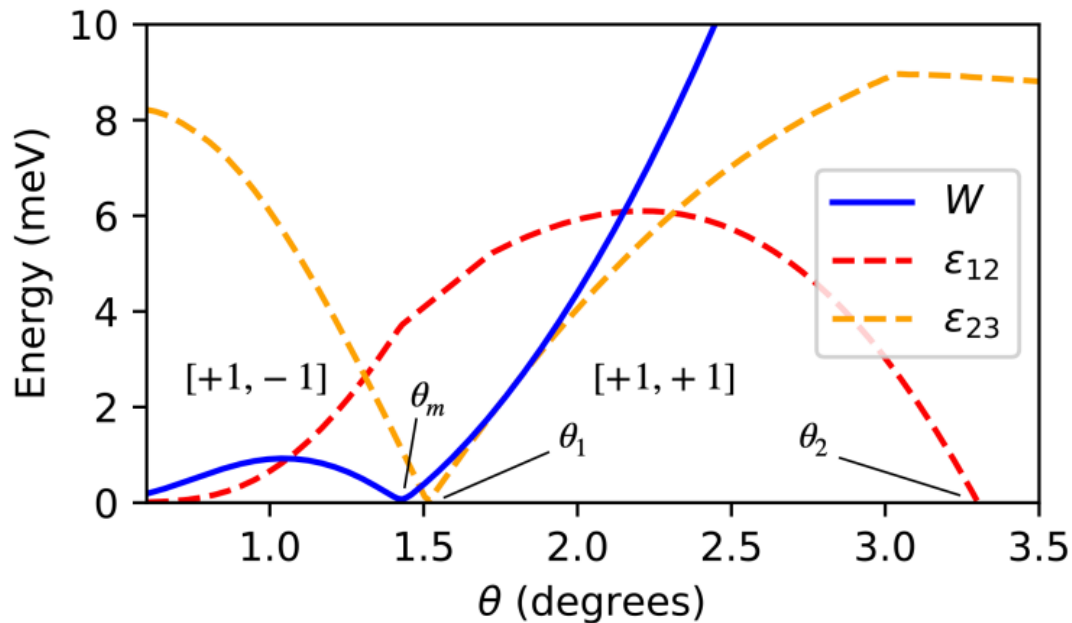


Correlated insulator at $n=1$:

- valley-polarized (Ising) ferromagnet
- intervalley coherent (xy) antiferromagnet

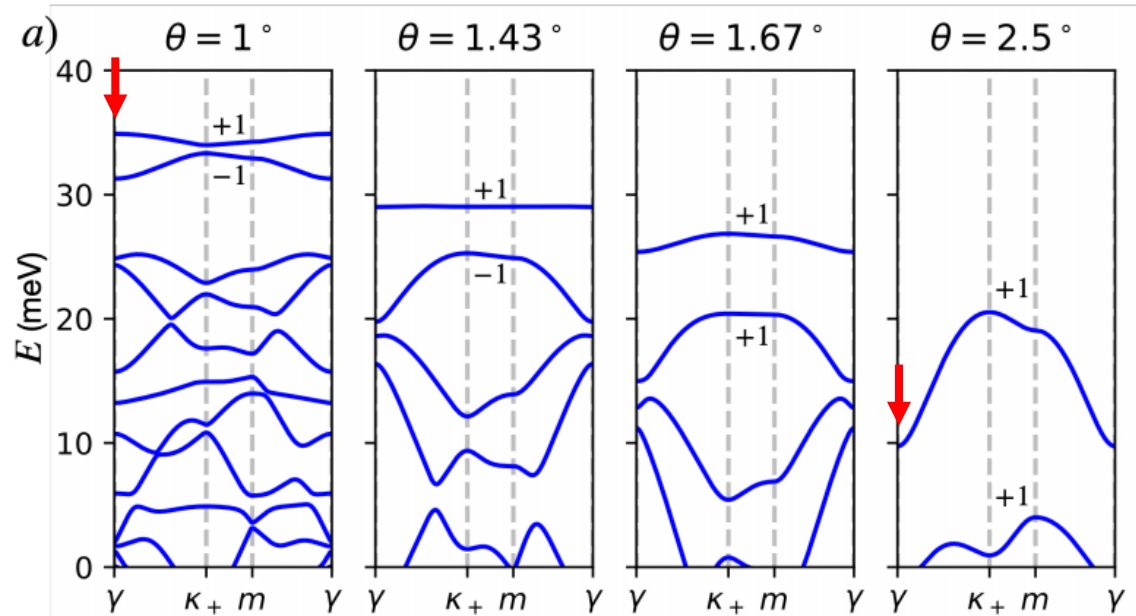
Bi & LF, Nature Communications (2021)
See also Cano & Millis, Das Sarma ...

Isolated Topological Bands



Devakul, Crepel, Zhang & LF, Nature Communications (2021)

$\theta \sim 1.4^\circ$: Magic *Flat Band*



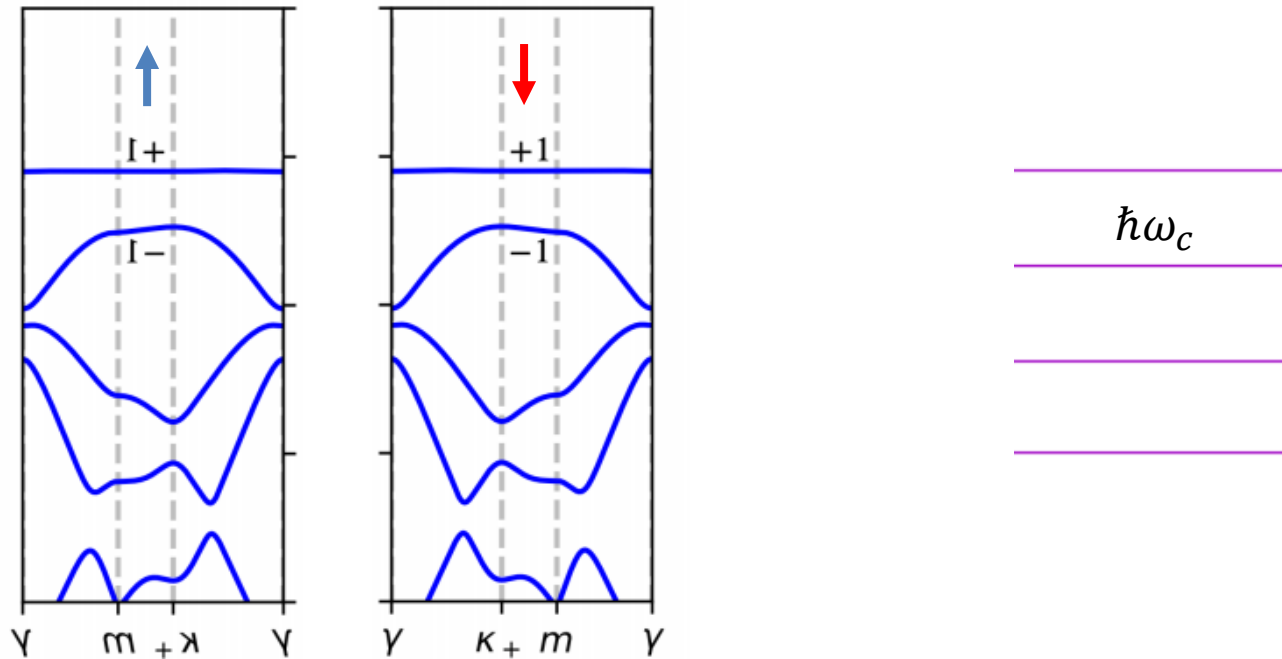
Analytical formula for **magic angle** based on diverging band mass at γ

$$\tilde{\theta}_m^{-2} = \frac{8\pi^2}{9m^*a_0^2} \left(\frac{1}{\mathcal{E}_{n_0} - \mathcal{E}_{n_0+1}} + \frac{1}{\mathcal{E}_{n_0} - \mathcal{E}_{n_0-1}} \right)$$

$$\text{where } \mathcal{E}_n = 2w \cos(\pi n/3) + 2V \cos(2\pi n/3 - \psi),$$

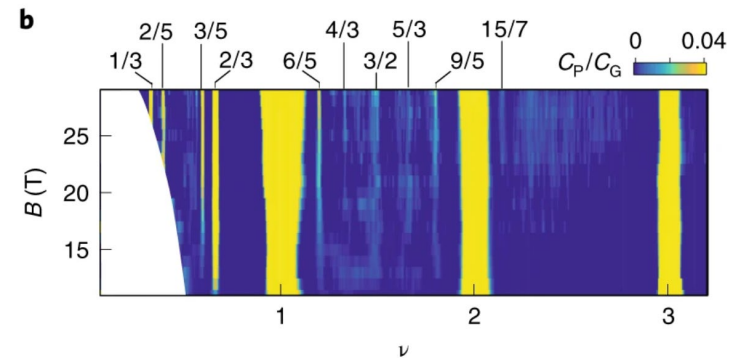
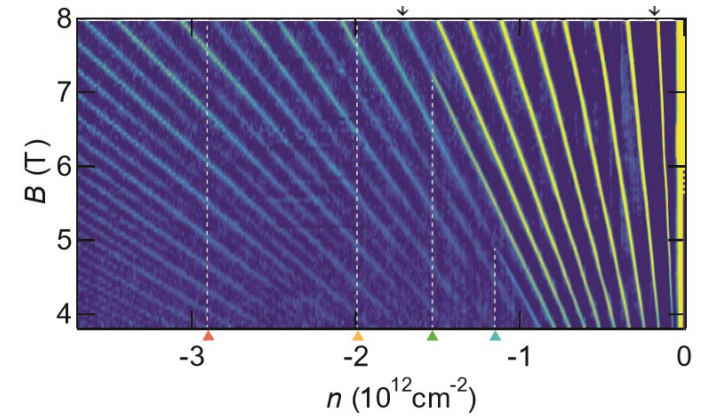
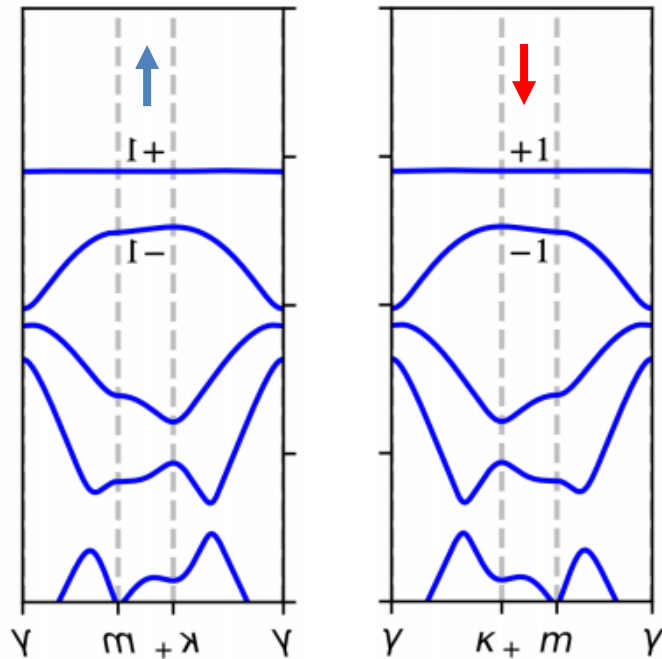
Magic flat band: bandwidth 0.1meV, topological gap 4meV

Comparison with Landau Level



Topological gap 4meV $\Leftrightarrow B = 18\text{T}$ in monolayer WSe₂

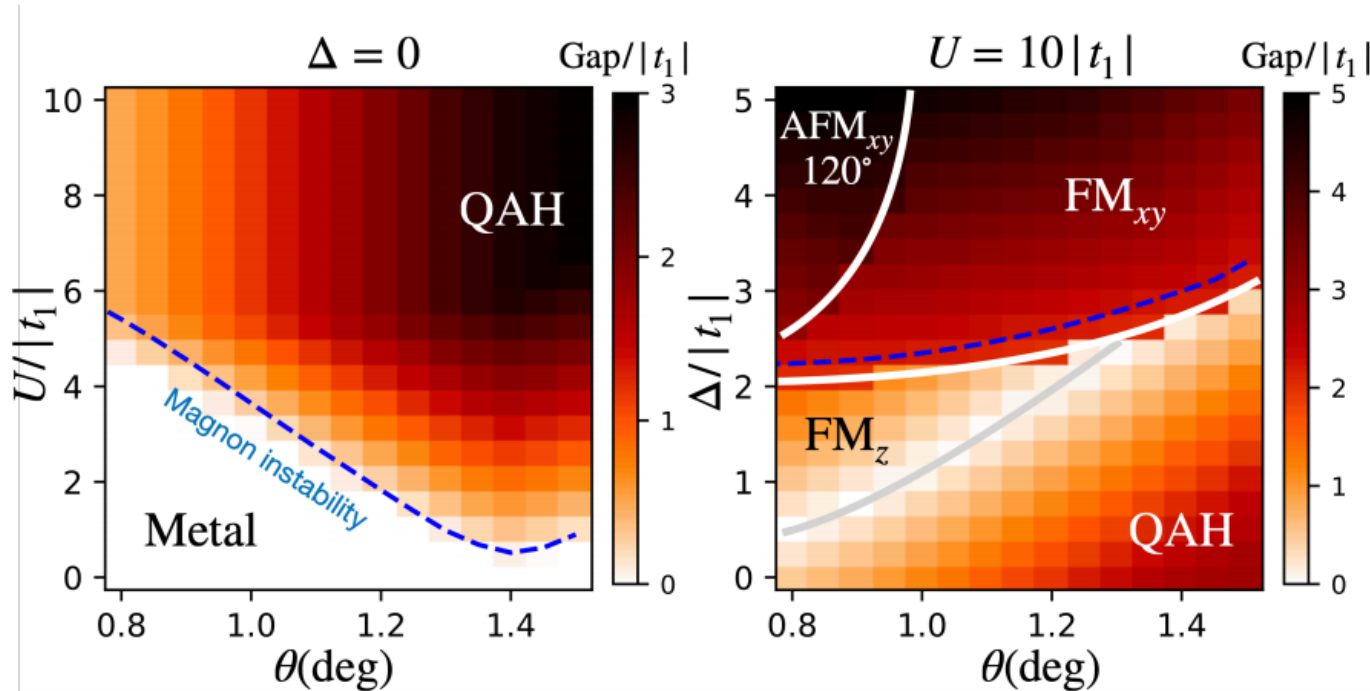
Comparison with Landau Level



Shi et al, Nat. Nano. 2020

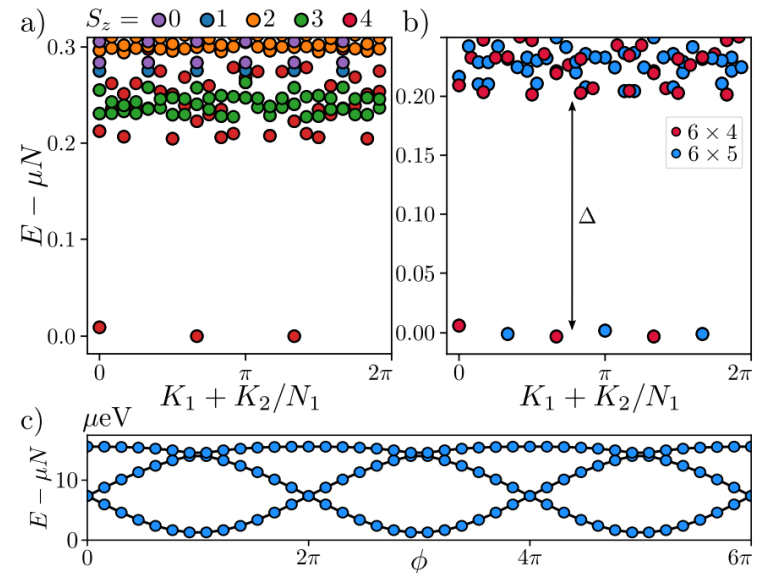
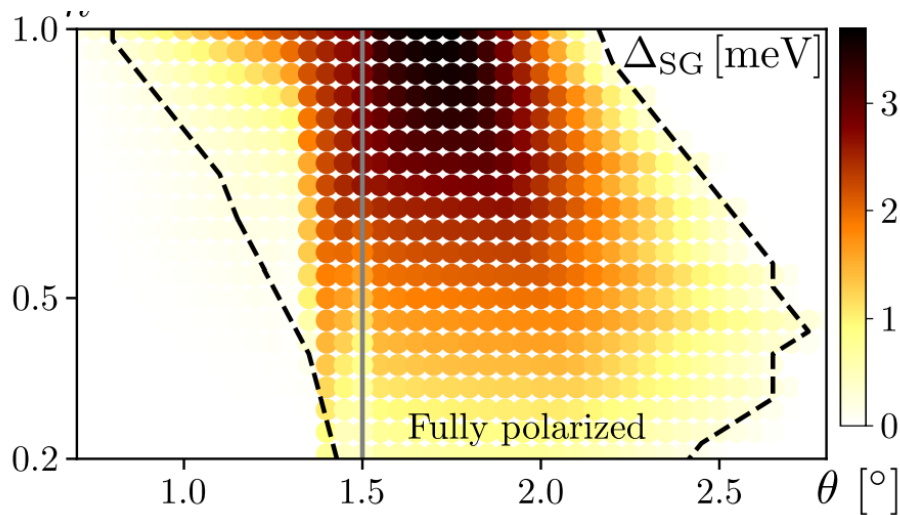
Topological gap 4meV $\Leftrightarrow B = 18\text{T}$ in monolayer WSe_2

Haldane and Mott Insulators at $n=1$ tuned by electric field



Devakul, Crepel, Zhang & LF, Nature Communications (2021)

Fractional Fillings: Anomalous Hall Metal & Fractional Chern Insulator

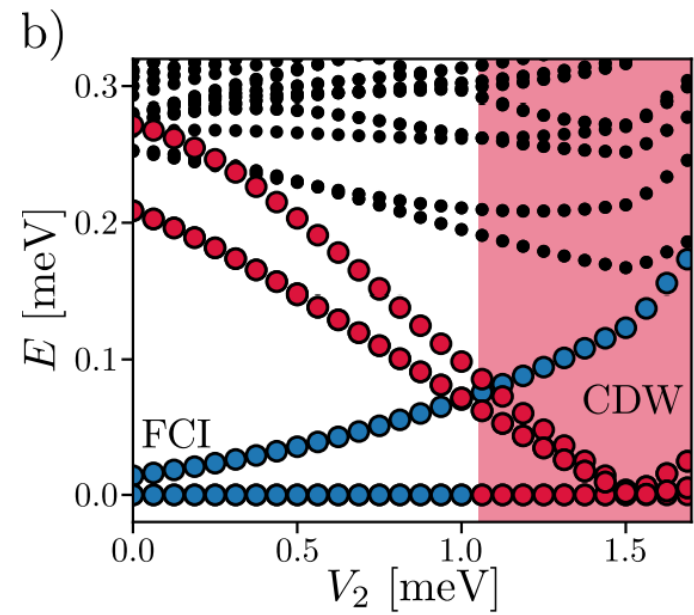
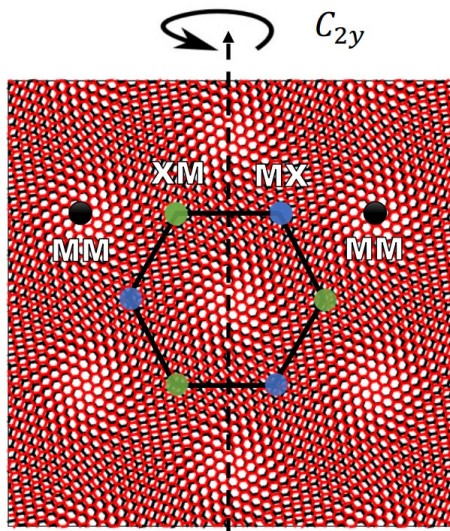


Spontaneous spin-valley polarization
Gapped magnon due to spin-valley locking

Crepel & LF, arXiv:2207.08895

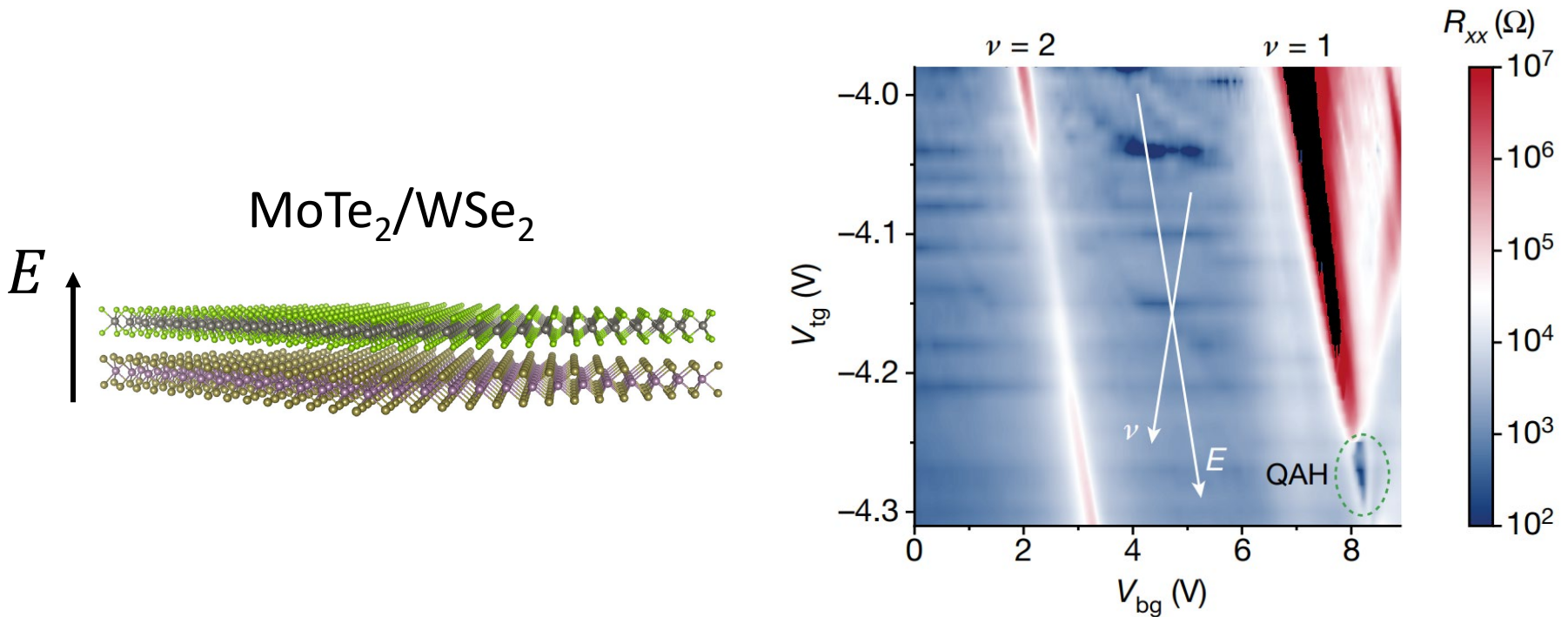
See also Li, Kumar, Sun and Lin, Physical Review Research 3, L032070 (2021).

FCI vs CDW



Quantum anomalous Hall effect from intertwined moiré bands

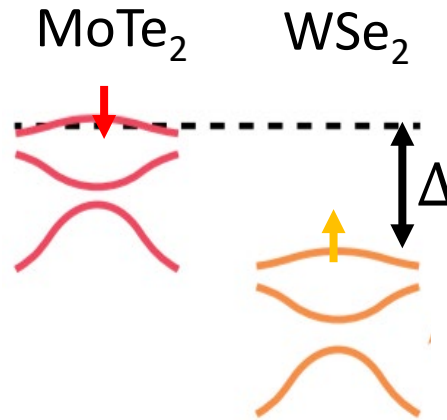
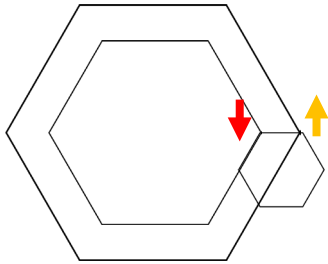
[Tingxin Li](#), [Shengwei Jiang](#), [Bowen Shen](#), [Yang Zhang](#), [Lizhong Li](#), [Zui Tao](#), [Trithep Devakul](#), [Kenji Watanabe](#), [Takashi Taniguchi](#), [Liang Fu](#), [Jie Shan](#)  & [Kin Fai Mak](#) 



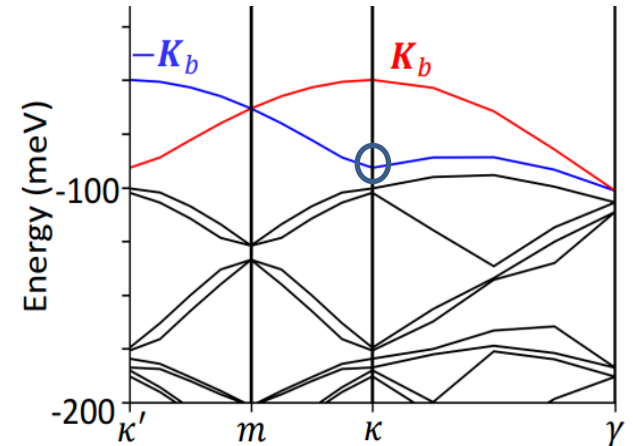
- Electric field tunes interlayer charge transfer

Moire Bands in MoTe₂/WSe₂

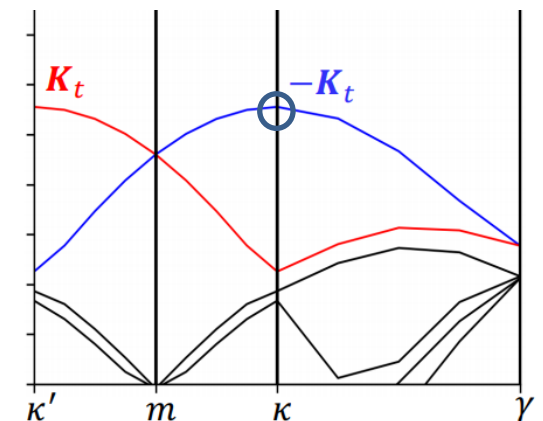
$$a_M = 4.6\text{nm}$$



13 x13 MoTe₂

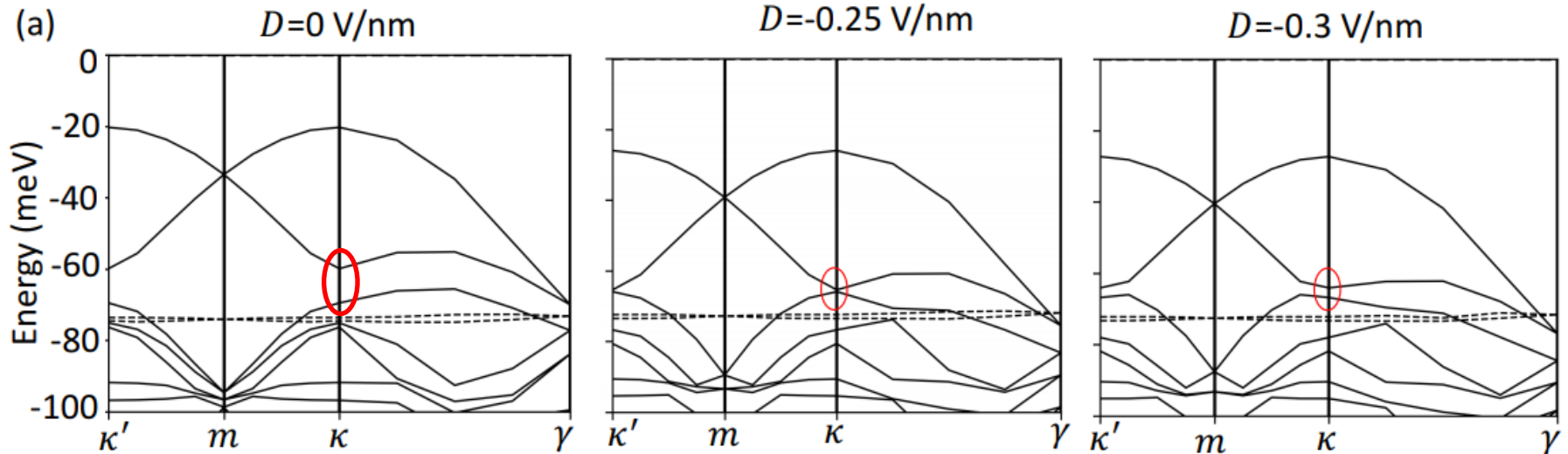


14 x14 WSe₂



- $\Delta = 0.13\text{eV}$ at zero E field
- majority layer: MoTe₂
minority layer: WSe₂
- moire band due to lattice corrugation with bandwidth $\sim 50\text{ meV}$

E Field Tunes Band Inversion

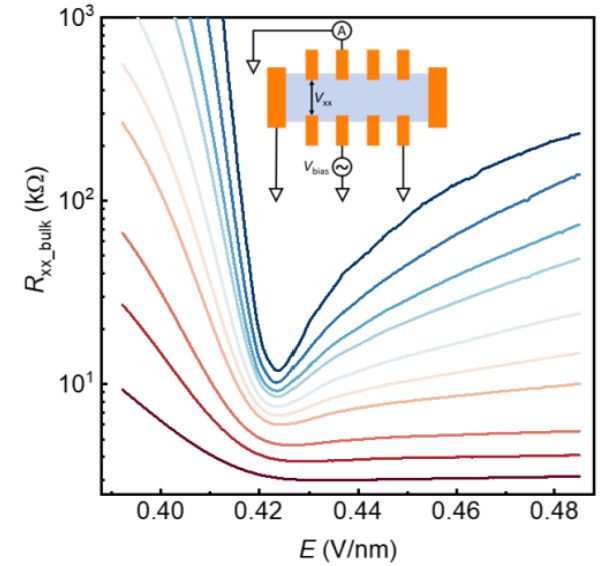
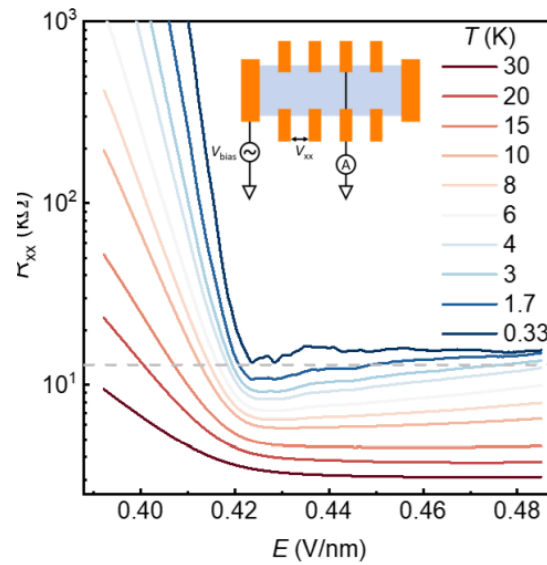
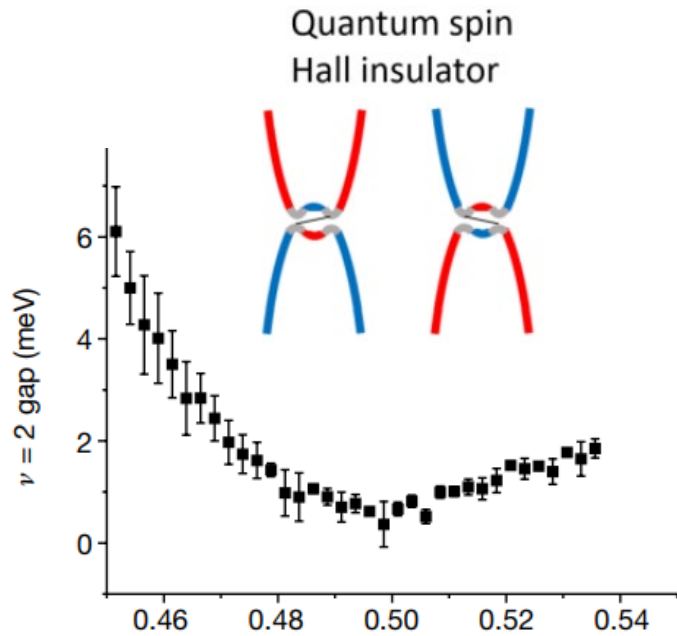


- electric field inverts minibands on two layers
- band inversion + p-wave interlayer tunneling \Rightarrow valley Chern number

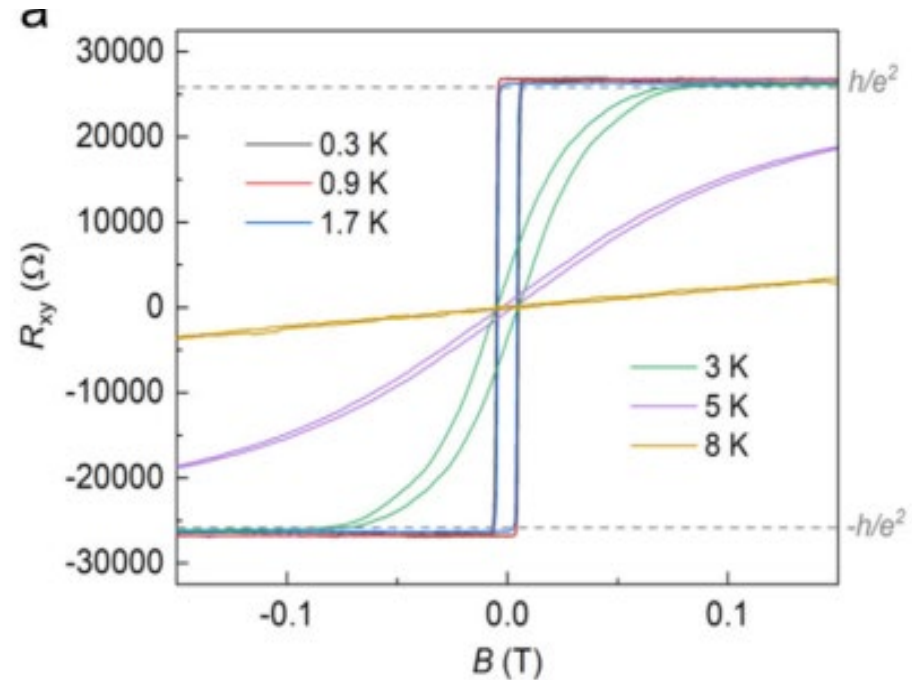
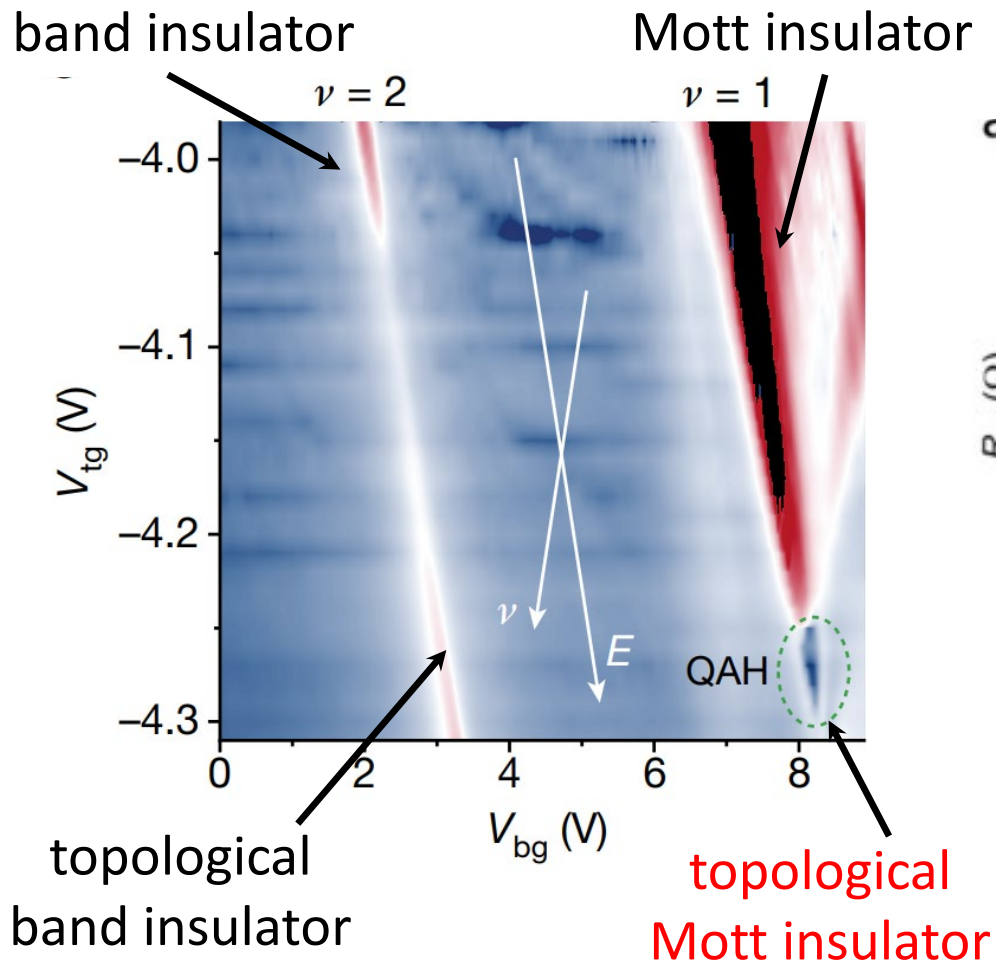
Prediction: E field induced quantum spin Hall insulator at $n=2$

Zhang, Devakul & LF, PNAS (2021)

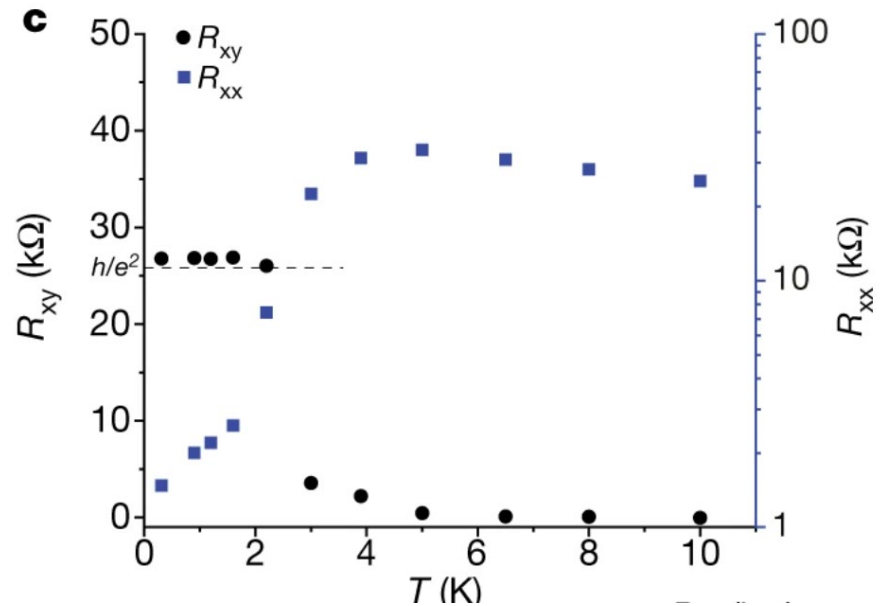
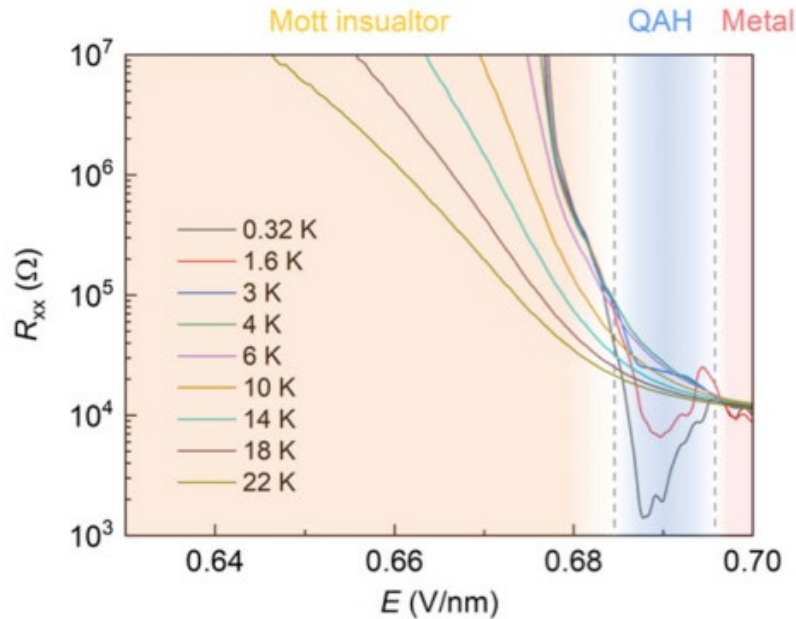
Edge Transport in MoTe₂/WSe₂



Quantum Anomalous Hall Effect at Half Filling



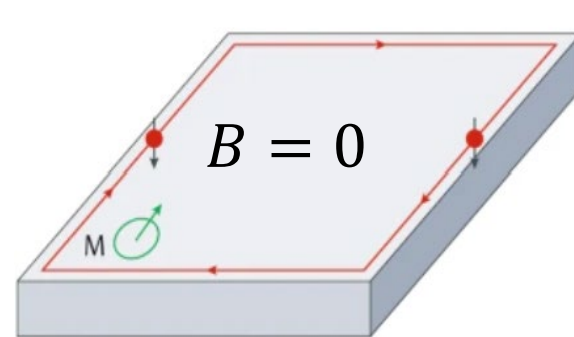
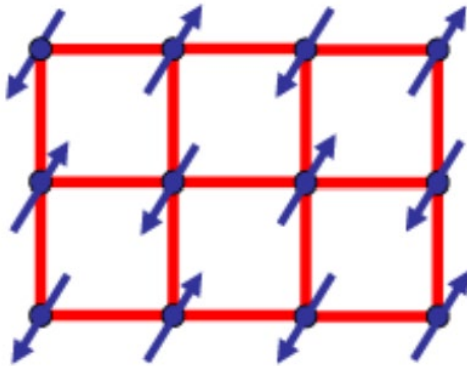
E Field Induced Mott-QAH Transition



- absence of E field hysteresis
- robust and reproducible

Mottness versus Topology

dichotomy between particle and wave



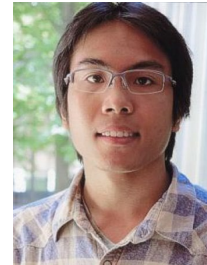
Mott

Topology



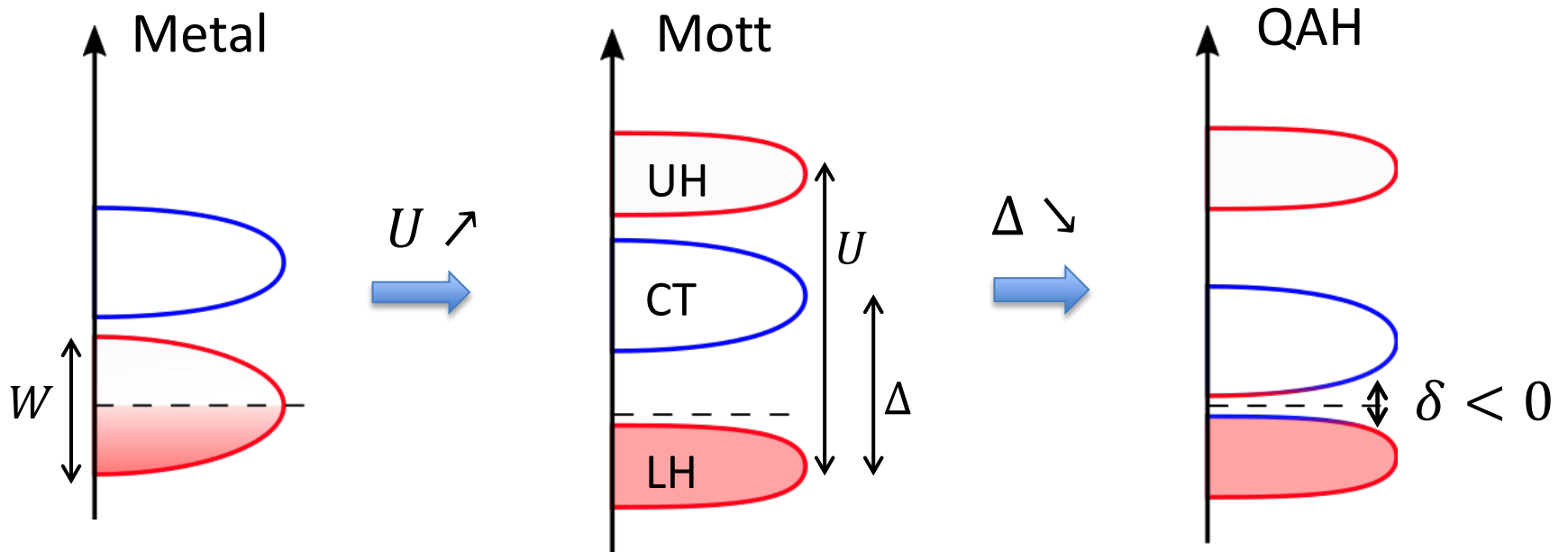
Quantum Anomalous Hall State in Antiferromagnetic Mott Insulators

Devakul & LF, PRX (2022)



Mott to QAH Insulators

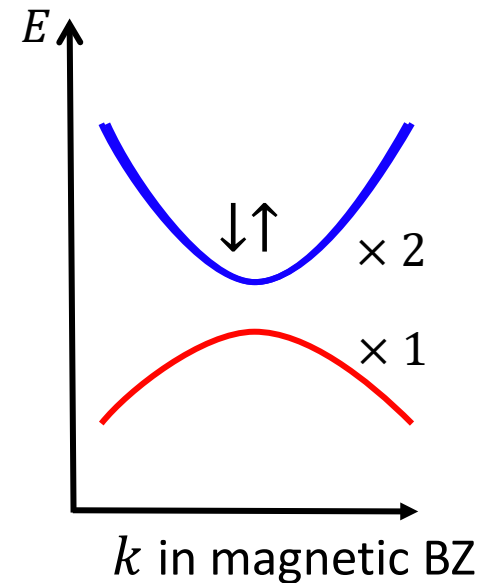
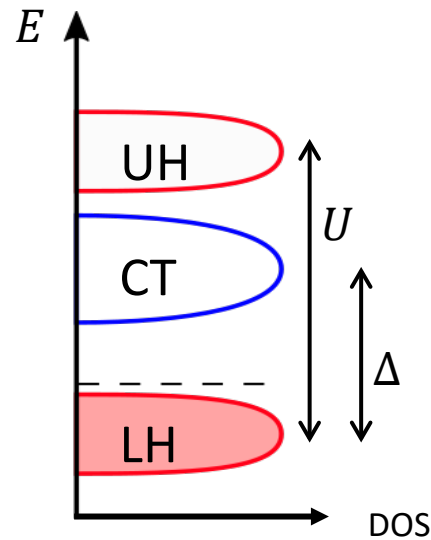
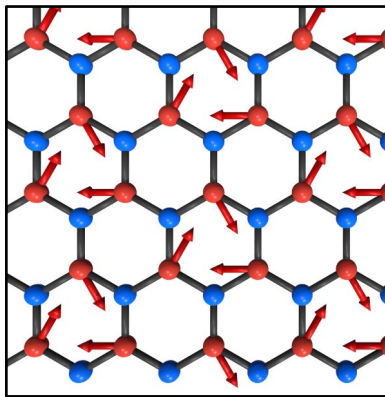
Mott-QAH transition by inverting charge transfer gap



Devakul & LF, PRX (2022)

$$\delta \sim \Delta - W$$

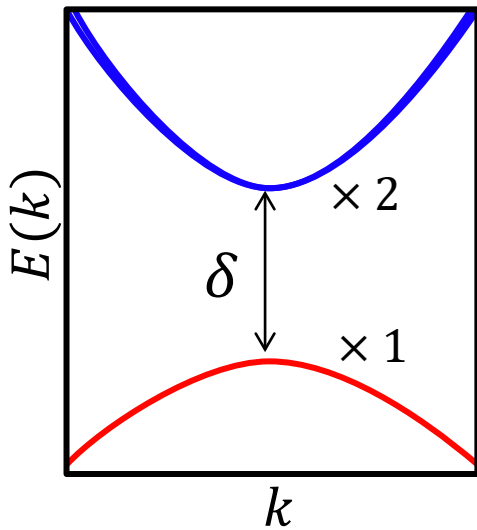
120°-AFM Mott Insulator



- Quasiparticle bands in magnetically ordered insulator are different from noninteracting bands.
- Low-energy states: **spin-polarized holes on majority layer** & **spin-degenerate electrons on minority layer**

Interacting Field Theory

$$\mathcal{H}_{\text{eff}} = \int \psi^\dagger H_{\text{eff}} \psi d\mathbf{k} + g \int n_{B\uparrow}(r)n_{B\downarrow}(r)dr \quad \psi = (\psi_A, \psi_{B\uparrow}, \psi_{B\downarrow})$$

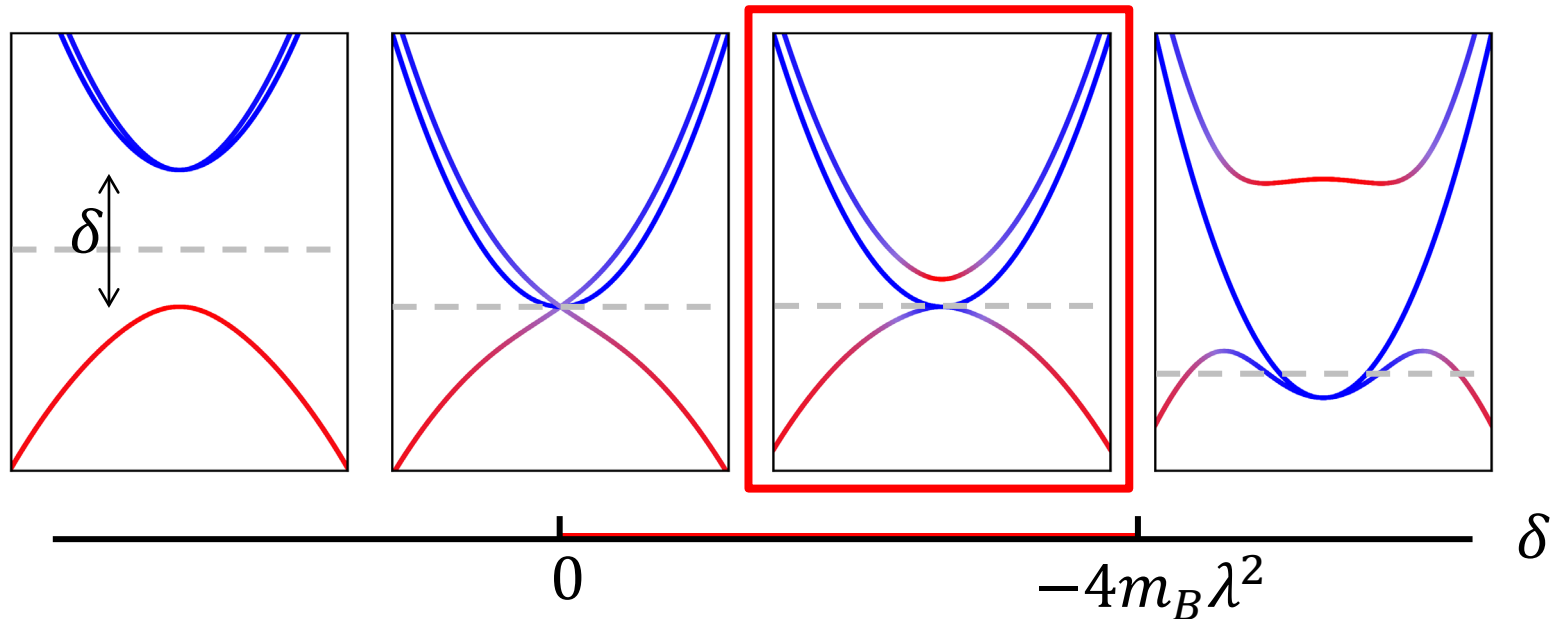


$$H_{\text{eff}} = \begin{pmatrix} -\frac{k^2}{2m_A} & \lambda(k_x + ik_y) & \lambda(k_x - ik_y) \\ " & \frac{k^2}{2m_B} + \delta & 0 \\ " & 0 & \frac{k^2}{2m_B} + \delta \end{pmatrix}$$

- spin degeneracy at $k=0$ on minority layer protected by C_3 & Ts_z
- p-wave hybridization dictated by band symmetry
- g : electron repulsion on minority layer

Interacting Field Theory

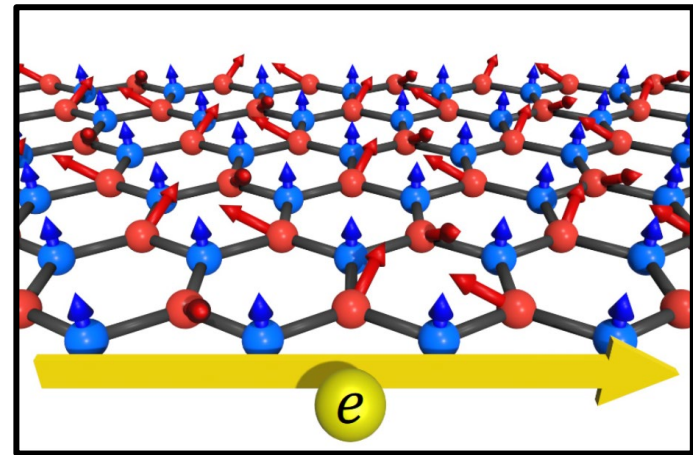
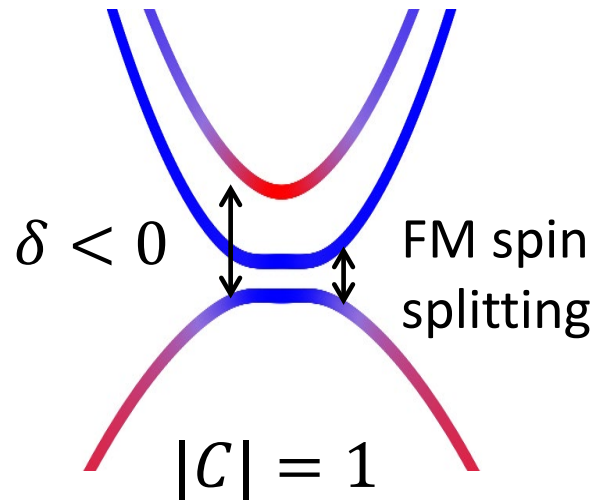
Quasiparticle band at $g = 0$



After band inversion $\delta < 0$, quadratic band touching appears at Fermi level, which is unstable to repulsion g [Sun, Yao, Fradkin, Kivelson, PRL 2009](#)

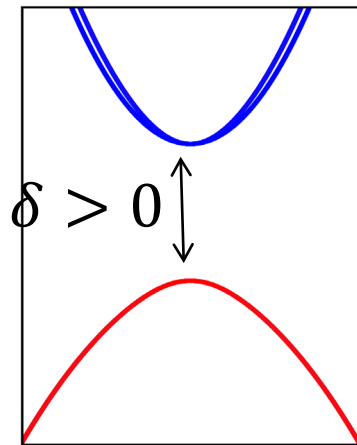
$g > 0$ changes from irrelevant to marginally relevant at band inversion, enabling an unconventional continuous Mott-QAH transition.

QAH with non-coplanar magnetism

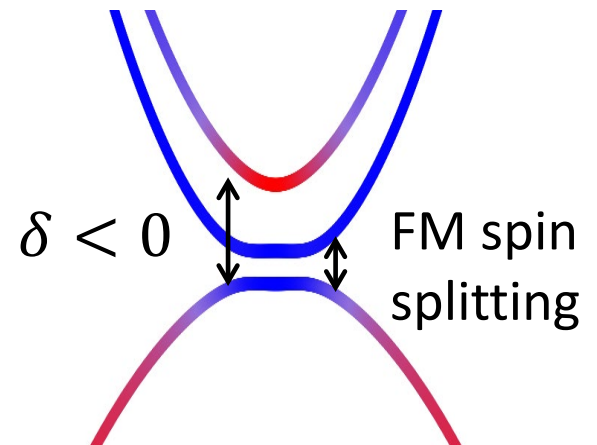
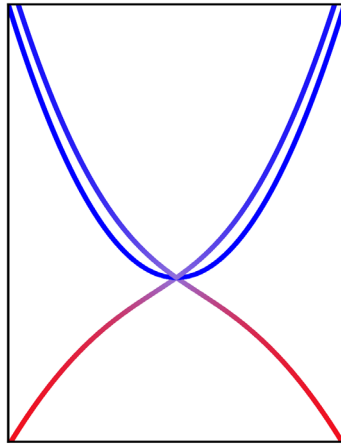


- After quasiparticle band inversion, Ising FM in minority layer opens Chern gap at quadratic band touching
- chiral spin order: xy-AFM in MoTe_2 & Ising FM in WSe_2
- canting of xy-AFM allowed by symmetry

Continuous Mott-Chern Transition



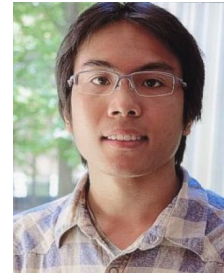
$$C = 0$$



$$|C| = 1$$

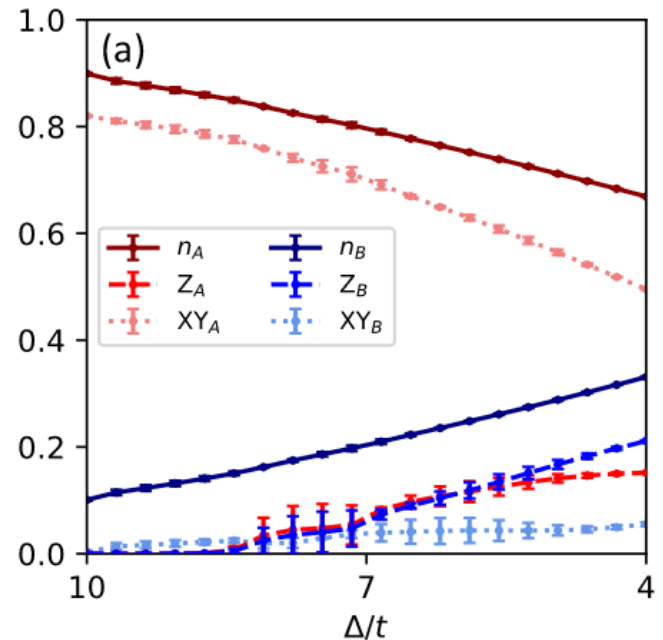
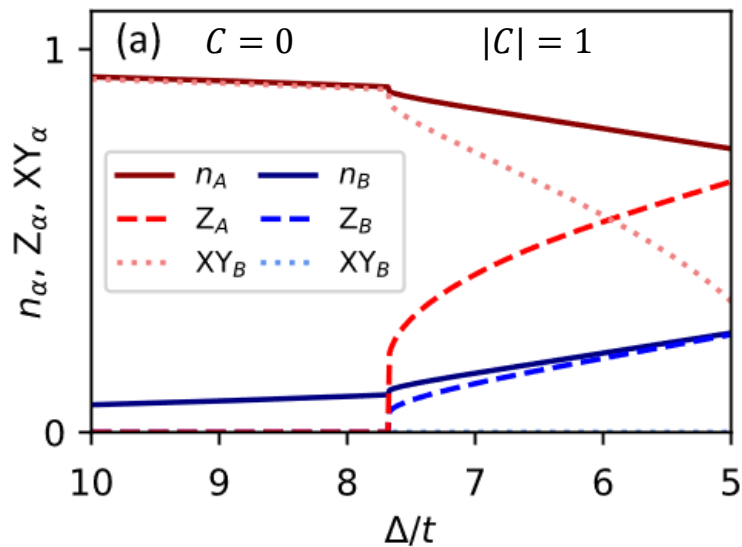
Inverting charge transfer gap induces simultaneous change of magnetism & topology.

Numerical Results



Self-consistent Hartree-Fock

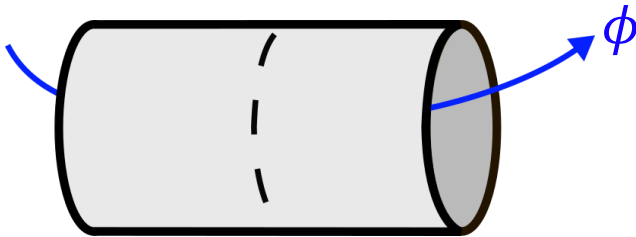
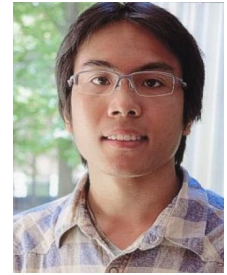
DMRG



Honeycomb Hubbard model

$$H = H_A + H_B + H_{AB} + H_\Delta + H_U$$

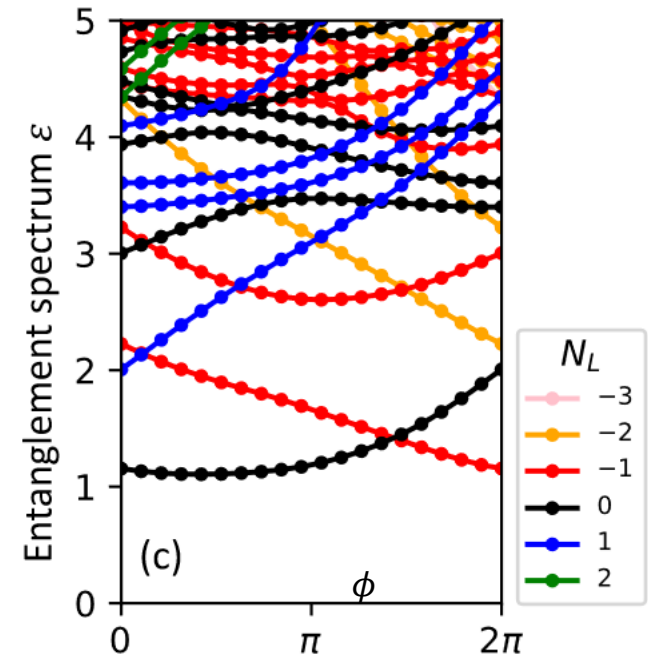
Topology in DMRG



Laughlin 1981.

Charge pumping argument

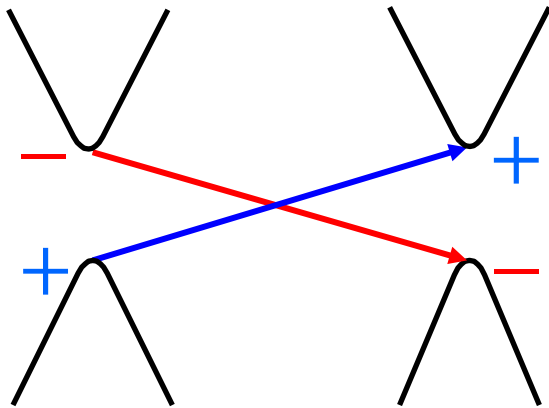
$$\sigma_{xy} = \frac{I_x}{V_y} = \delta_{N_L} \frac{e^2}{h} \Rightarrow |C| = 1$$



$$\begin{aligned} \phi &\rightarrow \phi + 2\pi \\ N_L &\rightarrow N_L - 1 \end{aligned}$$

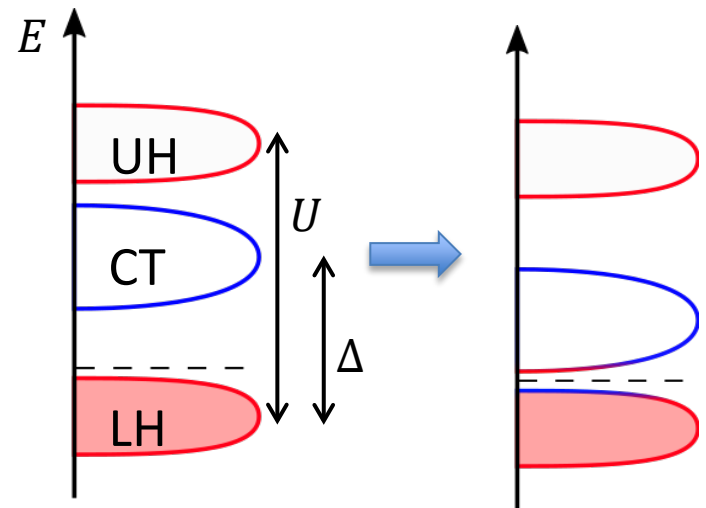
Topological Band & Mott Insulators

Inverting single-particle gap
(even-integer filling)



2007

Inverting many-body gap
(odd-integer filling)



2022

AFM Mott insulators with **negative** charge transfer gap:
potential route to high-temperature QAH

Bridging Mott and Chern



Comparison with Other QAH Systems

Magnetically doped TI film [Chang et al \(2013\)](#)

- FM of dopant opens Chern gap at surface Dirac point
- even integer filling

Magic-angle graphene [Sharpe et al, Serlin et al \(2019\)](#)

- fully valley-polarized flat Chern band

$$C_K = +1$$

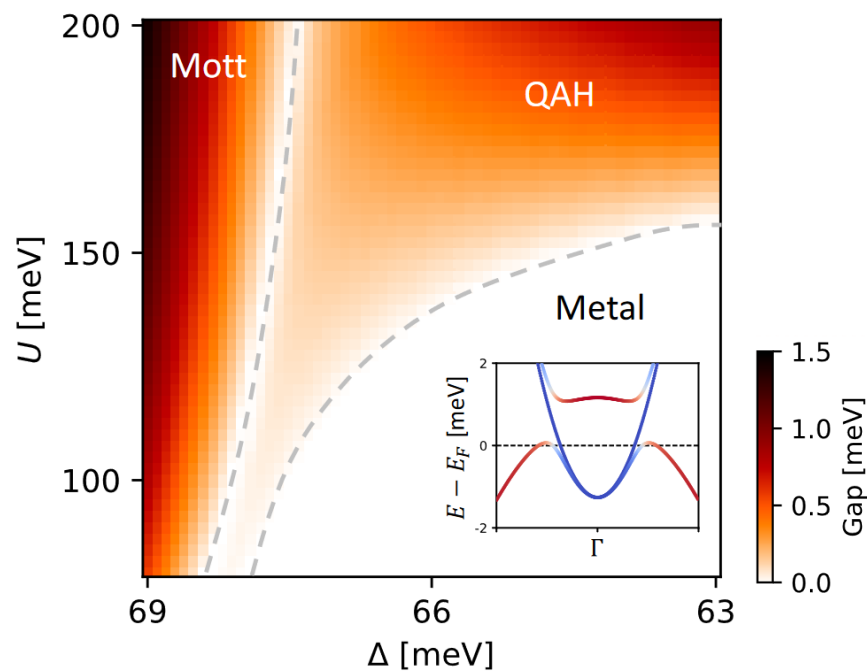

$$C_{K'} = -1$$


[Zhang & Senthil, MacDonald,
Xie et al, Pan et al ...](#)

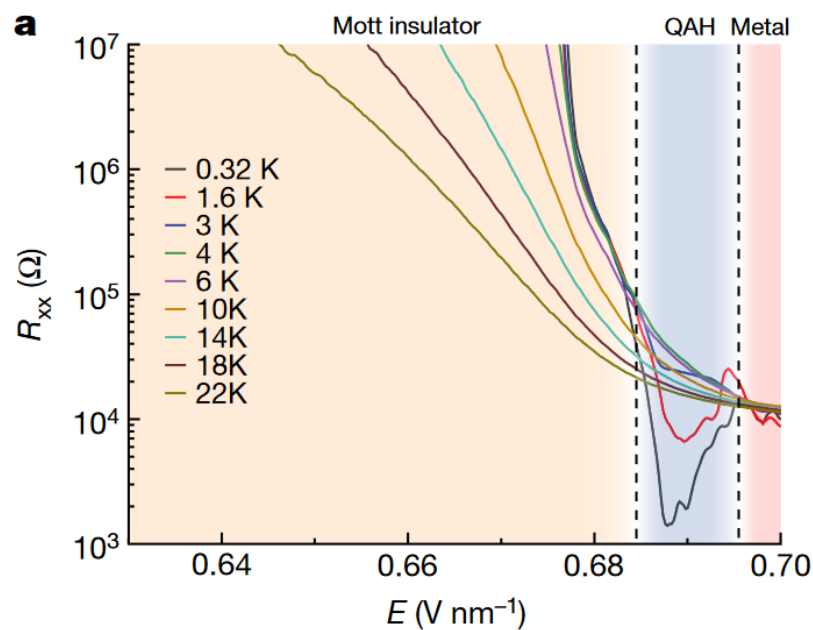
QAH in $\text{MoTe}_2/\text{WSe}_2$ differs fundamentally from flat band FM.

Comparison with Experiment

Hartree-Fock Phase Diagram



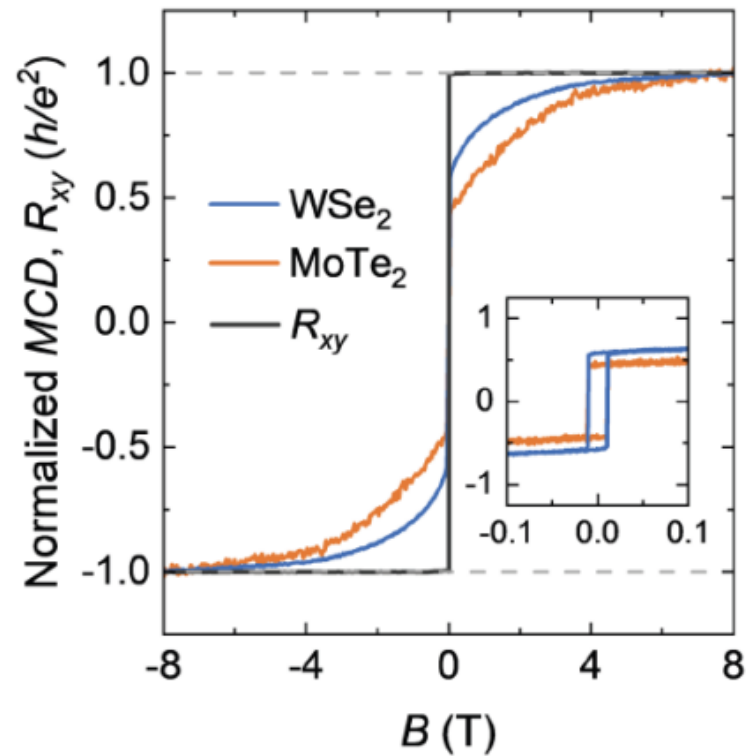
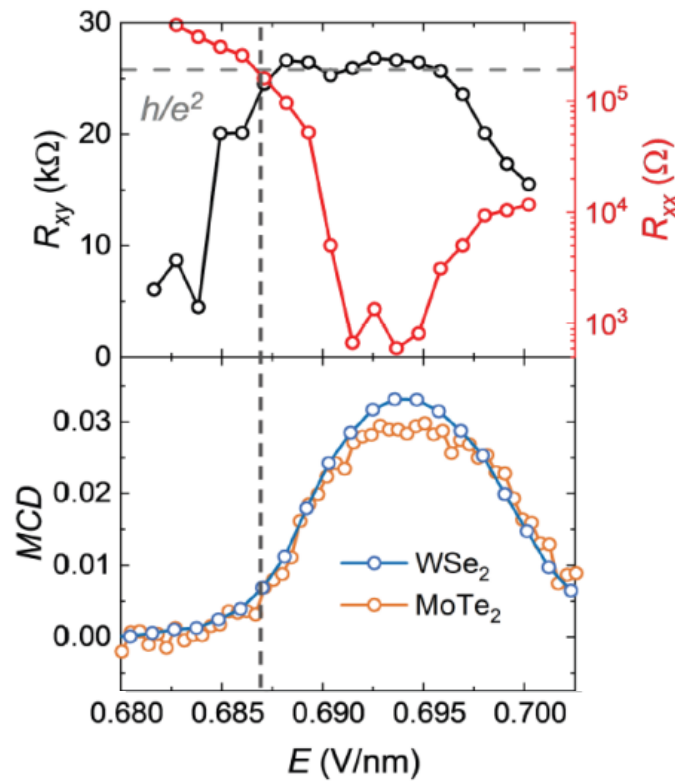
MoTe₂/WSe₂



Prediction for Magnetism

- Mott: **zero** spin S_z polarization
- QAH: **finite but incomplete** spin S_z polarization increasing with B field and E field
- Intervalley *XY* magnetic order: **gapless** magnon

Evidence for Canted Spin Texture in QAH



Outlook

- charge gap across Mott-Chern transition
- spin superfluidity
- critical exponents
- inverting quantum spin liquid

Theory

Yang Zhang

Noah Yuan

Bi Zhen

Hiroki Isobe

Trithep Devakul

Philip Crowley

Nisarga Paul

Valentin Crepel

Margarita Davydova

Aidan Reddy

Kevin Slagle (Caltech)

Junkai Dong (Cornell)

Jie Wang (Flatiron)

Experiment

Kin Fai Mak & Jie Shan (Cornell)

Feng Wang (Berkeley)

Xiaodong Xu (UW Seattle)

Ben Feldman (Stanford)

Pablo Jarillo-Herrero



SIMONS
FOUNDATION